Received: 4 January 2022 | Revised: 30 January 2022 | Accepted: 6 February 2022

DOI: 10.1002/bio.4207

RESEARCH ARTICLE

LUMINESCENCE WILEY
The Journal of Biological and Chemical Luminescence

# Highly sensitive biosensor based on aptamer and hybridization chain reaction for detection of cadmium ions

Mingming Xu[1] | Yu Peng[1] | Hualin Yang[1,2] | Yu Zhou[1,3]

[1]Institute of Food Science and Technology, College of Life Science, Yangtze University, 266 Jingmi Road, Jingzhou, Hubei, China

[2]State Environmental Protection Key Laboratory of Synergetic Control and Joint Remediation for Soil &Water Pollution, Chengdu University of Technology, Chengdu, Sichuan, China

[3]College of Animal Science, Yangtze University, 266 Jingmi Road, Jingzhou, Hubei, China

**Correspondence**
Hualin Yang and Yu Zhou, Institute of Food Science and Technology, College of Life Science, Yangtze University, 266 Jingmi Road, Jingzhou, Hubei, 434025, China.
Email: yanghualin2005@126.com;
Email: zhouyurunye@sina.com

**Funding information**
State Environmental Protection Key Laboratory of Synergetic Control and Joint Remediation for Soil &Water Pollution, Grant/Award Number: GHBK-2020-001; National Natural Science Foundation of China, Grant/Award Numbers: 31601536, 31871888

## Abstract

In this work, a highly sensitive biosensor for detecting cadmium ions ($Cd^{2+}$) was developed based on a $Cd^{2+}$-specific DNA aptamer and a hybridization chain reaction (HCR). The $Cd^{2+}$ aptamer (named S0) was used to recognize $Cd^{2+}$ and trigger the HCR. Without $Cd^{2+}$, S0 initiated the HCR to form long nicked dsDNA structures to quench the fluorescence. Then, $Cd^{2+}$ could bind with S0 to block HCR to recover fluorescence. This biosensor had high sensitivity with a detection limit of 0.36 nM and a linear range from 0 to 10 nM. Moreover, it showed a satisfactory selectivity and recovery rates.

**KEYWORDS**
aptamer, biosensor, cadmium ions, HCR, high sensitivity

## 1 | INTRODUCTION

Heavy metal pollution is a huge concern due to high toxicity and persistence.[1,2] Among the heavy metals, cadmium ions ($Cd^{2+}$) are considered one of the most extreme toxic metal ions for humans. Environmental exposure to $Cd^{2+}$ can cause serious health issues involving many serious diseases and various types of cancers.[3–6] The major problem is the wide utilization of $Cd^{2+}$ in different daily processes such as agricultural practices, industrial production, and public life. Moreover, due to its long metabolic half-life, $Cd^{2+}$ is easily bio-accumulated in animals and human beings through the food chain.[7,8] European legislation has set a limit of 0.3–0.5 mg/L for $Cd^{2+}$ discharge into the environment.[9] In addition, the World Health Organization (WHO) and United States Environment Protection Agency (US EPA) have defined the maximum permissible limits of 3 μg/L and 5 μg/L for $Cd^{2+}$ in drinking water, respectively. Therefore, quantitative determination of $Cd^{2+}$ at trace or even ultra-trace concentrations is of great significance in environmental chemistry.

The traditional methods for $Cd^{2+}$ determination rely on instrument analysis including inductively coupled plasma mass spectrometry (ICP-MS),[10] and atomic absorption spectroscopy.[11] Although these methods are sensitive and accurate, they require expensive instruments or complicated procedures. Recently, large numbers of new methods have been reported to overcome the shortcomings of traditional methods. According to the chemical nature of the recognition group, these methods can be divided into organic small molecule probes,[3,12,13] protein probes,[14] nanomaterial probes[15,16], and DNA probes.[17–19] However, in these methods, new problems were exposed such as the complex synthesis of the probes. Because DNA is commercial, chemically stable, and easy to modify, DNA methods stand out.[20–22]

Aptamers are single-stranded DNA oligonucleotides with a specific nucleic acid sequence that has high affinity and specificity

  

towards a wide range of target molecules.[23] Since its discovery, aptamers for many targets such as ATP, thrombin, and cocaine have been screened. On this basis, various detection methods have been established.[23] For $Cd^{2+}$, the first $Cd^{2+}$ aptamer was selected in 2014 by the Zhou group.[19] They designed a $Cd^{2+}$ biosensor based on the aggregation of gold nanoparticles (AuNPs) with a detection limit of 4.6 nM. Although this method has high sensitivity due to the high affinity of the aptamer for $Cd^{2+}$, its sensitivity could still be improved by an amplification strategy. Subsequently, many methods have been developed for detecting $Cd^{2+}$ based on a $Cd^{2+}$ aptamer.[24–26] To improve sensitivity, many signal amplification strategies have been applied including polymerase chain reaction (PCR),[27] exonuclease III (Exo III)[ digestion,[28] and hybridization chain reaction (HCR). Among them, HCR is an enzyme-free amplification technique using DNA self-assembly that is triggered by an initiator DNA and leads to the formation of long nicked double-stranded DNA structures under mild conditions. This technique was first introduced by Dirk and Pierce.[29] Subsequently, it became a fascinating and effective amplification strategy to detect DNA,[30] proteins,[31] cells,[32] small molecules,[33] and various heavy metal ions.[34–37] In this work, we used HCR to improve the sensitivity and a combined $Cd^{2+}$-specific DNA aptamer as a recognizer to ensure the specificity.

## 2 | EXPERIMENTAL

### 2.1 | Reagents and apparatus

Metal ions ($CdCl_2$, $HgCl_2$, AgCl, $BaCl_2$, $CuSO_4$, $ZnSO_4$, $Pb(NO_3)_2$, $FeCl_3$, NaCl, $MnCl_2$, $NiCl_2$, $MgSO_4$, $CrCl_3$, $CoCl_2$) were purchased from Sinopharm Chemical Reagent Co., Ltd. Other reagents were purchased from Aladdin Co., Ltd (Shanghai, China). All chemicals were of analytical grade. The aqueous solutions were prepared with deionized water (resistance 18.2 MΩ.cm) that was obtained from a Milli-Q water purification system. The HPLC-purified DNA oligonucleotides used in this study were synthesized and purchased from Sangon Biological Engineering Technology and Services Co., Ltd (Shanghai, China) and their sequences are listed in Table 1. A stock solution of the oligonucleotides (100 μM) was prepared and stored at −20°C.

Fluorescence intensity was tested with a SpectraMax iD3 Multi-Mode Microplate Reader (USA). The excitation wavelength was 470 nm, the emission wavelengths were 510–650 nm, and the photomultiplier tube (PMT) detector voltage was set at a low voltage. Polyacrylamide gel electrophoresis (PAGE) was conducted on a voltage type electrophoresis imaging system (JY04S-3C, Beijing, China).

### 2.2 | Fluorometric analysis

Before the experiment, S1 and S2 were pretreated to form a hairpin structure by means of heating and cooling. Initially, 10 μM S1 and S2 was added into HEPES buffer (50 mM, NaCl 0.5 M, pH 8.0). Then, the solutions were heated to 95°C for 5 min and allowed to slowly cool down to room temperature within 2 h.

The titration of $Cd^{2+}$ was performed by adding different concentrations of $Cd^{2+}$ into HEPES buffer (50 mM, NaCl 0.5 M, pH 8.0) containing 20 nM S0. Then the samples were incubated at room temperature for 0.5 h to ensure the completion of the S0–$Cd^{2+}$ reaction. Next, according to a typical procedure,[38] 100 nM S1 and 100 nM S2 were added. The mixture was incubated at room temperature for 0.5 h to ensure signal stabilization. Finally, the fluorescence signals were measured on a SpectraMax iD3 Multi-Mode Microplate Reader.

The selectivity of the proposed method for $Cd^{2+}$ was evaluated by adding 10 nM $Cd^{2+}$ and 200 nM other interfering substances ($Mg^{2+}$, $Cu^{2+}$, $Pb^{2+}$, $Fe^{3+}$, $Ca^{2+}$, $Zn^{2+}$, $Mn^{2+}$, $Ni^{2+}$, $Ag^{+}$, $Co^{2+}$, $Ba^{2+}$, $Hg^{2+}$). The procedure was similar to that for the $Cd^{2+}$ titration experiment. The reaction volumes of all experiments were 100 μl.

### 2.3 | Gel electrophoresis analysis

PAGE was used to estimate the HCR process. Initially, 12% PAGE gel, and 1× Tris–borate–EDTA electrophoresis buffer (TBE, pH 8.0) were prepared. In addition, gel electrophoresis samples including the HCR product and different controls were prepared by adding loading buffer. Then, electrophoresis was performed at 140 V for ~40 min at room temperature. Finally, nucleic acid was stained using M5 Hipure Next III Gelred (DNA dye).

## 3 | RESULTS AND DISCUSSION

### 3.1 | Mechanism of the method

The principles of the $Cd^{2+}$-specific DNA aptamer and HCR amplified assay are shown in Scheme 1. Initially, three oligonucleotide probes S0, S1, and S2 were designed. Among them, S0 was used as the $Cd^{2+}$-specific DNA aptamer and the promoter for HCR. S1 and S2 can form hairpin structures separately at the beginning of the reaction. In this stage, hairpin S1 was labelled with a quencher (BHQ1), and hairpin S2 was labelled with 5-carboxyfluorescein (FAM), which can emit intense

**TABLE 1** Sequences of DNA used in this work

| DNA sequence (5′→3′) | |
|---|---|
| S0 | GGACTGTTGTGGTATTATTTTTGGTTGTGC |
| S1 | CCAAAAATAATACCACAACAGTCC/BHQ1/CAAAGTGGACTGTTGTGGTATTAT |
| S2 | GGACTGTTGTGGTATTATTTTTGGATAATACCACAACAGTCCACTTTG/FAM/ |

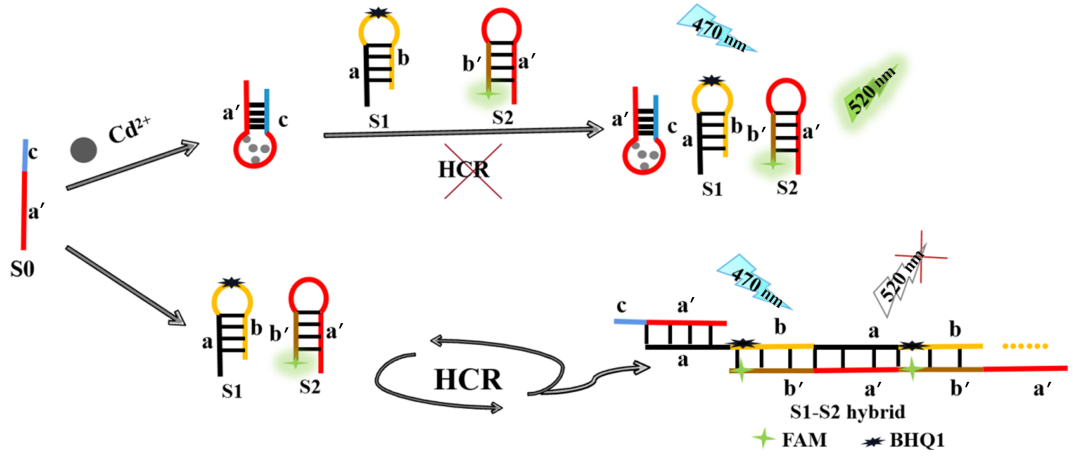


**SCHEME 1** Principles of the biosensor detection of $Cd^{2+}$

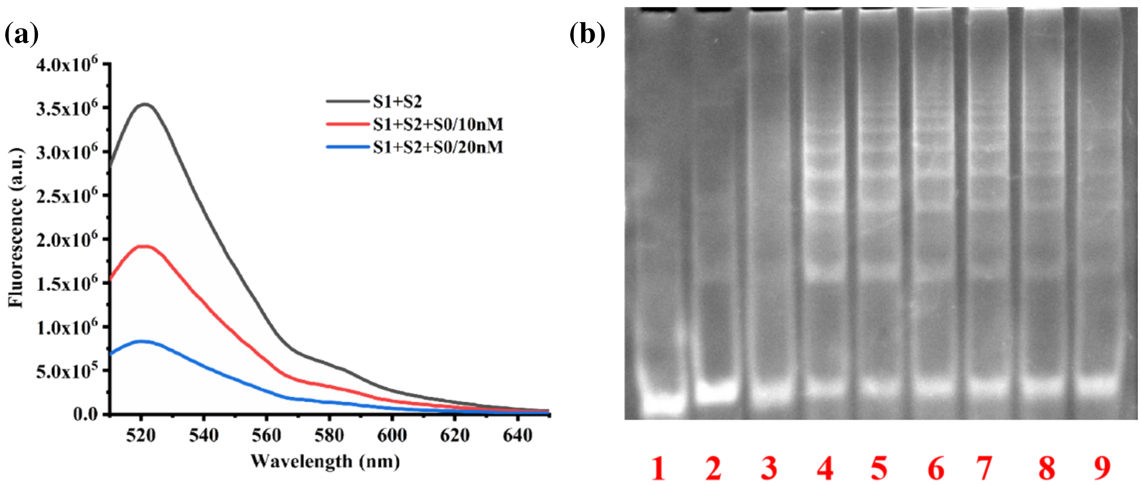


**FIGURE 1** (a) Fluorescence spectra under different treatment conditions: S1 + S2 (black), S1 + S2 + 10 nM S0 (red), S1 + S2 + 20 nM S0 (blue). (b) Native gel electrophoretic analysis (12% PAGE) of the HCR process under different S0 concentrations. Lane 1, S1; lane 2, S2; lane 3, S1 + S2; lane 4, S1 + S2 + 100 nM S0; lane 5, S1 + S2 + 50 nM S0; lane 6, S1 + S2 + 40 nM S0; lane 7, S1 + S2 + 30 nM S0; lane 8, S1 + S2 + 20 nM S0; lane 9, S1 + S2 + 10 nM S0. Concentrations of S1 and S2 in all the reaction systems were 100 nM

fluorescence. In addition, part a′ (red) of S0 was complementary to part a (black) of S1. Part b (yellow) of S1 was complementary to part b′ (brown) of S2.

In the absence of $Cd^{2+}$, S0 was free. It can hybridize to S1 by a–a′ interaction to open the hairpin structure of S1. Then, part b of S1 was released to hybridize with S2 through b–b′ In this case, hairpin S2 was opened and part a′ was released. Then part a′ of S2 can bind with the next S1 and trigger cascade hybridization of S1 and S2. Finally, a long double-stranded DNA (dsDNA) assembly polymer with multiple repeated units was formed. In this polymer, FAM, and BHQ1 were pulled close together, which resulted in the fluorescence quenching of FAM. In the presence of $Cd^{2+}$, free S0 was exhausted due to formation of the $Cd^{2+}$-aptamer complex.[19] Therefore, the HCR process could not occur. The distance between FAM and BHQ1 was far enough to avoid interference. Therefore, FAM fluorescence was recovered.

## 3.2 | The initialization of HCR by S0

According to the principle of the $Cd^{2+}$ biosensor, HCR was the key of this $Cd^{2+}$ biosensor. Therefore, S0 triggering of the HCR process was verified firstly. When merely S1 and S2 existed, an intense fluorescence signal could be observed (Figure 1a, black curve). When S0 was added, the fluorescence intensity was decreased significantly (Figure 1a, red curve). As the concentration of S0 doubled, fluorescence intensity decreased further, proportionally (Figure 1a, blue curve). These results indicated that S0 could successfully initiate the HCR.

To further confirm the principles of the $Cd^{2+}$ biosensor, gel electrophoretic analysis was used. The results are shown in Figure 1(b). Lanes 1, 2, and 3 correspond to S1, S2, and S1 + S2, respectively. Due to the lack of S0, the HCR cannot start, so the molecular weight was relatively small. When S0 was added, as shown in Figure 1(b), lane

4, some new bands can be seen clearly in the high-molecular-weight region. This result meant that the HCR was triggered. As multiple HCRs occurred and the degree of reaction was different, bands of different sizes were observed. As the concentration of S0 decreased gradually, the brightness of the bands decreased accordingly (lanes 4–9). These results further confirmed that the HCR in this work was triggered by S0.

### 3.3 | Optimization of HCR conditions

The HCR conditions were optimized to achieve better results. First, reaction buffers were optimized by comparing four different kinds of buffers (Tris–HCl, PBS, HEPES, and MOPS). As shown in Figure 2(a), HEPES buffer (purple) had a lowest F/F0 value and indicated that the HCR was the best. Moreover, this advantage remained constant over long periods. Therefore, HEPES buffer was chosen for subsequent experiments. In addition, ionic strength usually played an important role in the hybridization reactions. Ionic strength was studied by adding different concentrations of NaCl. Without NaCl, only a small amount of fluorescence quenching could be observed. When 0.5 M NaCl was added, a significant change in F/F0 was observed. As the concentration of NaCl continued to increase, the F/F0 value was close to that of the 0.5 M NaCl group (Figure 2b). Therefore, economically, 0.5 M NaCl can ensure the completion of the HCR. The reaction time was another important parameter. The HCR under different time periods was also investigated. The results showed that the HCR completed in 0.5 h.

### 3.4 | Optimization of S0 concentration

If the concentration of S0 was too low, it was not enough to initiate the HCR. However, if S0 was excessive, more $Cd^{2+}$ than expected

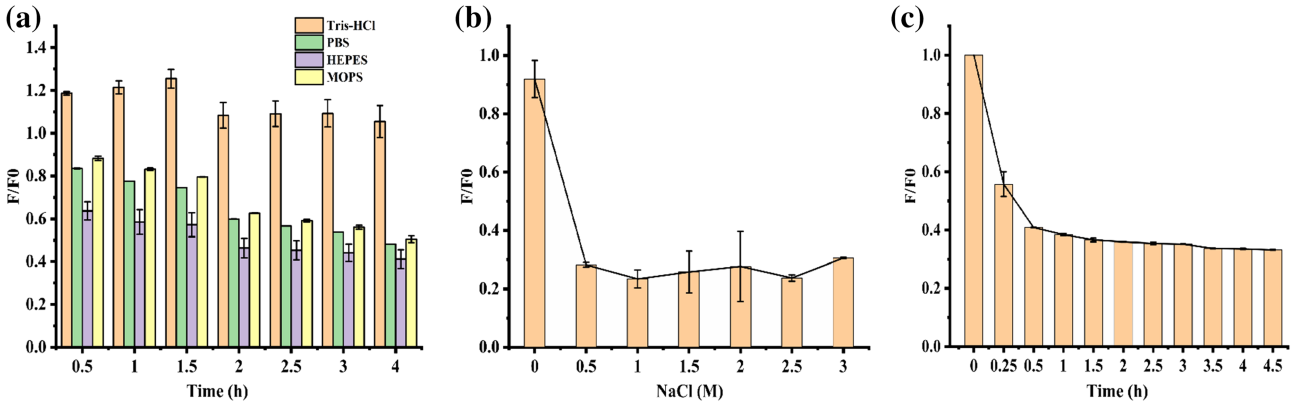


**FIGURE 2** (a) Fluorescence change (F/F0) in different buffers (Tris–HCl, PBS, HEPES, and MOPS) under different reaction time conditions. All buffers were 50 mM, pH 8.0. F and F0 were the fluorescence intensities in the presence or absence of S0, respectively. (b) Change of F/F0 under different concentrations of NaCl in HEPES buffer (50 mM, pH 8.0). (c) Change of F/F0 under different reaction time conditions

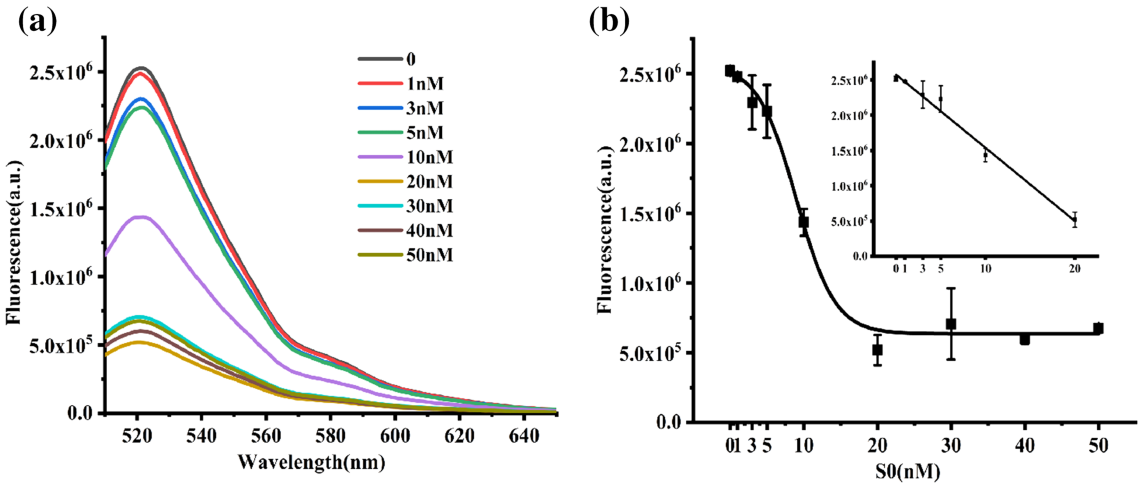


**FIGURE 3** (a) Fluorescence spectra of the HCR in the presence of different concentrations of S0. (b) Peak fluorescence intensity under different S0 concentrations. Inset: the linear relationship between fluorescence and S0 from 0 to 20 nM. Error bars represent the relative standard deviation of three repeated measurements

would be consumed to decrease the sensitivity of biosensor. For better $Cd^{2+}$ detection, S0 concentration titration experiments were performed. As shown in Figure 3(a), the fluorescence intensity of FAM decreased gradually with the increase of S0 from 0 to 20 nM. This result indicated that the HCR process was highly associated with the S0 concentration. Then, the fluorescence intensity reached a plateau. Even if the concentration of S0 was increased to 50 nM, the change in fluorescence intensity was not obvious. Considering that excessive S0 would reduce the sensitivity of the method, 20 nM S0 was chosen for the subsequent experiments. Subsequently, the peak fluorescence intensity was studied for quantitative analysis (Figure 3b). A linear correlation between the fluorescence intensity and the S0 concentration was found from 0 to 20 nM (inset of Figure 3b). The linear equation was $Y = 2.576 \times 10^6 - 103{,}848\ X$, $R^2 = 0.994$, where $Y$ and $X$ represent the fluorescence intensity and S0 concentration, respectively. The detection limit for DNA was estimated to be 0.96 nM based on the 3α/slope. This result implied that the concentration of $Cd^{2+}$ can be quantified by the binding relationship between $Cd^{2+}$ and S0.

## 3.5 | Feasibility for $Cd^{2+}$ detection

With the optimized HCR conditions, the feasibility of biosensor for $Cd^{2+}$ detection was studied. Because S0 was the $Cd^{2+}$ aptamer, it can be consumed with the addition of $Cd^{2+}$ by forming a $Cd^{2+}$–S0 complex. Therefore, the fluorescence of FAM can be recovered to respond to $Cd^{2+}$. As shown in Figure 4(a), the fluorescence intensity of the HCR increased with 3 nM $Cd^{2+}$. When the concentration of $Cd^{2+}$ was as high as 10 nM, the fluorescence increased further. These results suggested that it was feasible to detect $Cd^{2+}$ with our biosensor.

## 3.6 | Sensitivity of $Cd^{2+}$ biosensor

The sensitivity of biosensor was measured using a $Cd^{2+}$ titration experiment. As shown in Figure 4(b), in the concentration range 0–10 nM $Cd^{2+}$, the fluorescence intensity increased rapidly. This result suggested that S0 was used up by forming the Cd–S0 complex. Then the fluorescence intensity reached a plateau. Subsequently, even if the concentration of $Cd^{2+}$ continued to increase to 70 nM, the fluorescence intensity increase was not significant (Figure 4b). This suggested that $Cd^{2+}$ was saturated. In addition, there was a good linear relationship between fluorescence intensity and $Cd^{2+}$ concentration in the range 0–10 nM (inset of Figure 4b). The linear equation was $Y = 924{,}535 + 53{,}753\ X$ ($R^2 = 0.991$), where $Y$ and $X$ corresponded to the fluorescence intensity and $Cd^{2+}$ concentration, respectively. The detection limit was estimated to be 0.36 nM (~0.017 μg/L) based on the 3α/slope, which was two orders of magnitude lower than the US EPA defined level of $Cd^{2+}$ in drinking water (5 μg/L). The results indicated that this new biosensor could be used to detect $Cd^{2+}$ in aqueous solution with high sensitivity.

## 3.7 | Selectivity of $Cd^{2+}$ biosensor

Selectivity, as another indispensable factor, was researched by comparing the signal changes in the presence of different metal ions. The results showed that only $Cd^{2+}$ caused a marked signal change, whereas the other metal ions were all at the background level with slight changes even at 20 times concentrations of $Cd^{2+}$ (Figure 5). These results suggested that the new biosensor had a good selectivity for $Cd^{2+}$. The marked selectivity was due to the highly specific $Cd^{2+}$ aptamer complex. This result was identical to other reported method that also used a $Cd^{2+}$ aptamer to recognize $Cd^{2+}$.[39–42]

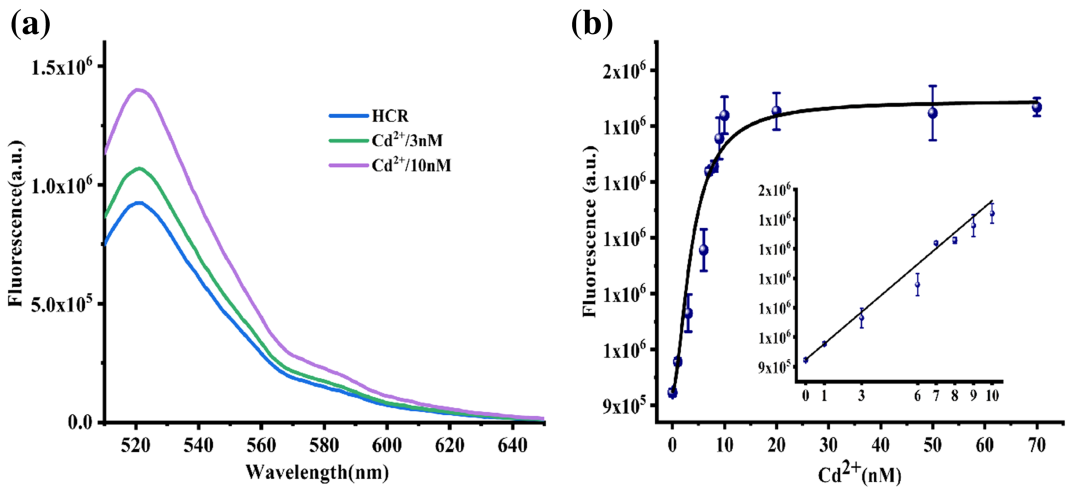


**FIGURE 4** (a) Fluorescence emission spectra under different conditions: S0 + S1 + S2 (blue), S0 + S1 + S2 + 3 nM $Cd^{2+}$ (green), S0 + S1 + S2 + 10 nM $Cd^{2+}$ (purple). (b) Fluorescence intensity changes of the proposed method in the presence of different concentrations of $Cd^{2+}$. Inset: the linear relationship between fluorescence intensity and the $Cd^{2+}$ concentration in the range 0–10 nM

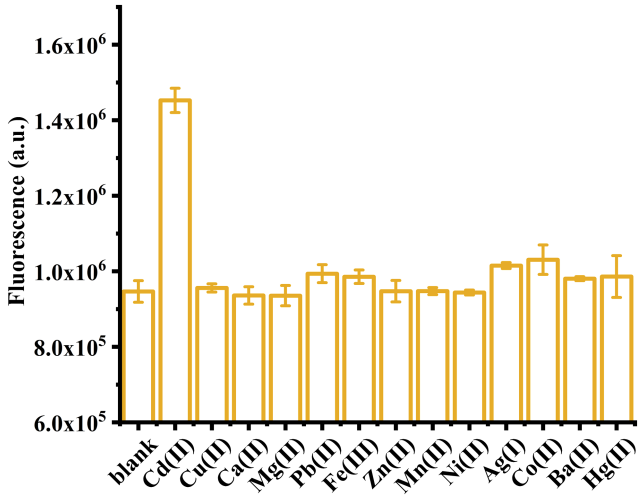


**FIGURE 5** Selectivity of the proposed method in the presence of 10 nM $Cd^{2+}$ and 200 nM interfering metal ions

**TABLE 2** Recovery experiments for the $Cd^{2+}$ biosensor in pond water

| Simple | Added $Cd^{2+}$ (nM) | Found (nM) | Recovery (%) |
|---|---|---|---|
| 1 | 0.00 | Not determinable | – |
| 2 | 3.00 | 3.04 ± 0.07 | 101.30 |
| 3 | 7.00 | 7.41 ± 0.49 | 105.86 |
| 4 | 9.00 | 8.74 ± 0.99 | 97.11 |

### 3.8 | Determination of $Cd^{2+}$ in pond water

To investigate the reliability and potential application of the proposed new biosensor, recovery experiments were carried out in pond water samples that were collected from Yangtze University. Different $Cd^{2+}$ concentrations of pond water samples were prepared by adding 3, 7 or 9 nM $Cd^{2+}$. Then, the level of $Cd^{2+}$ was measured using our method. In addition, pond water without added $Cd^{2+}$ was also tested as background. The results showed that the recovery rates were between 97.11% and 105.86% (Table 2). This satisfactory result suggested that our new method had potential application for $Cd^{2+}$ detection in real environmental samples.

## 4 | CONCLUSION

In summary, a new biosensor to detect $Cd^{2+}$ with high sensitivity and selectivity was developed based on an aptamer and the HCR. This biosensor did not need enzyme and complex synthesis steps. Due to the HCR amplification strategy, the biosensor was extremely sensitive with a detection limit of 0.36 nM that was two orders of magnitude lower than the US EPA defined level of cadmium in drinking water. The selectivity of this method was also very satisfactory due to the specific recognition of the $Cd^{2+}$-specific aptamer. In addition, this method showed good recovery rates for the detection of $Cd^{2+}$ in pond water. Therefore, this new biosensor had great potential to become a useful tool for detecting $Cd^{2+}$.

## ACKNOWLEDGEMENTS

The work is supported by the National Natural Science Foundation of China (31601536, 31871888), and State Environmental Protection Key Laboratory of Synergetic Control and Joint Remediation for Soil &Water Pollution (GHBK-2020-001).

## ORCID

*Hualin Yang* https://orcid.org/0000-0002-6439-9589

## REFERENCES

[1] X. Hu, X. Liu, X. Zhang, L. Cao, J. Chen, H. Yu, *Chemosphere* **2017**, *188*, 397.
[2] M. Vitkova, M. Puschenreiter, M. Komarek, *Chemosphere* **2018**, *200*, 217.
[3] L. Xue, G. Li, Q. Liu, H. Wang, C. Liu, X. Ding, S. He, H. Jiang, *Inorg. Chem.* **2011**, *50*, 3680.
[4] S. Satarug, M. R. Moore, *Environ. Health Perspect.* **2004**, *112*, 1099.
[5] M. P. Waalkes, T. P. Coogan, R. A. Barter, *Crit. Rev. Toxicol.* **1992**, *22*, 175.
[6] M. P. Waalkes, *J. Inorg. Biochem.* **2000**, *79*, 241.
[7] A. A. Tinkov, V. A. Gritsenko, M. G. Skalnaya, S. V. Cherkasov, J. Aaseth, A. V. Skalny, *Environ. Pollut.* **2018**, *235*, 429.
[8] J. Wen, G. Zeng, *J. Environ. Manage.* **2018**, *212*, 46.
[9] I. C. Santos, R. B. R. Mesquita, A. Rangel, *Talanta* **2015**, *143*, 359.
[10] Y. Qing, Y. Hang, R. Wanjaul, Z. Jiang, B. Hu, *Anal. Sci.* **2003**, *19*, 1417.
[11] J. Ning, Y. Jiao, J. Zhao, L. Meng, Y. Yang, *Water Sci. Technol.* **2014**, *70*, 605.
[12] H. N. Kim, W. X. Ren, J. S. Kim, J. Yoon, *Chem. Soc. Rev.* **2012**, *41*, 3210.
[13] S. Sarkar, R. Shunmugam, *ACS Appl. Mater. Interfaces* **2013**, *5*, 7379.
[14] A. Varriale, M. Staiano, M. Rossi, S. D'Auria, *Anal. Chem.* **2007**, *79*, 5760.
[15] Z. Wang, L. Li, E. Liu, *Thin Solid Films* **2013**, *544*, 362.
[16] Y. Zhang, Z. Zhang, D. Yin, J. Li, R. Xie, W. Yang, *ACS Appl. Mater. Interfaces* **2013**, *5*, 9709.
[17] P. J. Huang, J. Liu, *Nucleic Acids Res.* **2015**, *43*, 6125.
[18] H. Wang, H. Cheng, J. Wang, L. Xu, H. Chen, R. Pei, *Talanta* **2016**, *154*, 498.
[19] Y. Wu, S. Zhan, L. Wang, P. Zhou, *Analyst* **2014**, *139*, 1550.
[20] Z. Qing, J. Xu, J. Hu, J. Zheng, L. He, Z. Zou, S. Yang, W. Tan, R. Yang, *Angew. Chem., Int. Ed.* **2019**, *58*, 11574.
[21] J. Deng, J. Xu, M. Ouyang, Z. Zou, Y. Lei, J. Li, Z. Qing, R. Yang, *Chinese Chemical Letters*, Elsevier, China **2021**.
[22] H. L. Yang, Y. Zhou, J. W. Liu, *Trend Anal. Chem.* **2020**, *132*, 116060.
[23] M. Citartan, S. C. Gopinath, J. Tominaga, S. C. Tan, T. H. Tang, *Biosens. Bioelectron.* **2012**, *34*, 1.
[24] Y. F. Zhu, Y. S. Wang, B. Zhou, J. H. Yu, L. L. Peng, Y. Q. Huang, X. J. Li, S. H. Chen, X. Tang, X. F. Wang, *Anal. Bioanal. Chem.* **2017**, *409*, 4951.
[25] Y. X. Luan, A. X. Lu, J. Y. Chen, H. L. Fu, L. Xu, *Appl. Sci.-Basel* **2016**, *6*, 432.
[26] B. Zhou, X. Y. Yang, Y. S. Wang, J. C. Yi, Z. Zeng, H. Zhang, Y. T. Chen, X. J. Hu, Q. L. Suo, *Microchem. J.* **2019**, *144*, 377.
[27] Y. Peng, M. Xu, Y. Guo, H. Yang, Y. Zhou, *Spectrochim. Acta a Mol. Biomol. Spectrosc.* **2022**, *271*, 120885.
[28] L. W. Zeng, J. Y. Gong, P. S. Rong, C. S. Liu, J. H. Chen, *Talanta* **2019**, *198*, 412.

[29] R. M. Dirks, N. A. Pierce, *Proc. Natl. Acad. Sci. U. S. a.* **2004**, *101*, 15275.
[30] F. Xuan, I. M. Hsing, *J. Am. Chem. Soc.* **2014**, *136*, 9810.
[31] K. Peng, H. Zhao, Y. Yuan, R. Yuan, X. Wu, *Biosens. Bioelectron.* **2014**, *55*, 366.
[32] Y. M. Wang, Z. Wu, S. J. Liu, X. Chu, *Anal. Chem.* **2015**, *87*, 6470.
[33] B. Yang, X. B. Zhang, L. P. Kang, G. L. Shen, R. Q. Yu, W. Tan, *Anal. Chem.* **2013**, *85*, 11518.
[34] J. Huang, X. Gao, J. Jia, J. K. Kim, Z. Li, *Anal. Chem.* **2014**, *86*, 3209.
[35] M. Rana, E. E. Augspurger, M. S. Hizir, E. Alp, M. V. Yigit, *J. Mater. Chem. C* **2018**, *6*, 452.
[36] Y. Chen, L. Chen, Y. Ou, Z. Wang, F. Fu, L. Guo, *Talanta* **2016**, *155*, 245.
[37] J. Zhuang, L. Fu, M. Xu, Q. Zhou, G. Chen, D. Tang, *Biosens. Bioelectron.* **2013**, *45*, 52.
[38] Y. Jia, X. Shen, F. Sun, N. Na, J. Ouyang, *J. Mater. Chem. B* **2020**, *8*, 11074.
[39] C. S. Lee, S. H. Yu, T. H. Kim, *Microchem. J.* **2020**, *159*, 105372.
[40] S. Rabai, M. Benounis, G. Catanante, A. Baraket, A. Errachid, N. Jaffrezic Renault, J. L. Marty, A. Rhouati, *Anal. Biochem.* **2021**, *612*, 113956.
[41] Y. Liu, D. Zhang, J. Ding, K. Hayat, X. Yang, X. Zhan, D. Zhang, Y. Lu, P. Zhou, *Biosensors (Basel)* **2020**, *10*, 195.
[42] J. Chen, J. Pan, C. Liu, *Anal. Chem.* **2020**, *92*, 6173.

**How to cite this article:** M. Xu, Y. Peng, H. Yang, Y. Zhou, *Luminescence* **2022**, *37*(4), 665. https://doi.org/10.1002/bio.4207